Observed Low Frequency Variability of the Brazil Current Front

Gustavo Jorge Goni
National Oceanic and Atmospheric Administration
Atlantic Oceanographic and Meteorological Laboratory, Miami, Florida

Francis Bringas
Cooperative Institute for Marine and Atmospheric Studies
University of Miami, Miami, Florida

Pedro Nicolas DiNezio
Cooperative Institute for Marine and Atmospheric Studies
University of Miami, Miami, Florida

Corresponding author address: Gustavo Jorge Goni, National Oceanic and Atmospheric Administration, Atlantic Oceanographic and Meteorological Laboratory, 4301 Rickenbacker Causeway, Miami, FL 33149.
E-mail: Gustavo.Goni@noaa.gov

Abstract

The Brazil Current is a weak western boundary current, the southwest component of the South Atlantic subtropical gyre, which is the main conduit of upper ocean waters in the region. The objective of this work is to report on observed low frequency variability of the Brazil Current front using satellite-derived sea height anomaly and sea surface temperature observations during the 1993-2008 period is analyzed. The variability of the front is studied in terms of the separation of the Brazil Current front from the continental shelf break. During the study period, estimates of this parameter indicate a shift to the south of approximately 1.5 degrees. Simultaneously, the interior of the South Atlantic subtropical gyre exhibited an expansion of approximately 40% with the largest changes in the gyre are observed at it southern boundary about 35°S. Statistically significant changes are not observed in the geostrophic transport of the Brazil and Malvinas currents suggesting that the low-frequency changes of the Brazil Current front are governed by different mechanisms than the seasonal variability. Longer records together with comprehensive numerical experiments will ultimately be needed to determine the origin of these changes.

1. Introduction

The subtropical gyre is the dominant large-scale feature of the South Atlantic Ocean. This large-scale circulation comprises several components. The southern branch of the South Equatorial Current is the northern limb of the gyre, which bifurcates off Brazil at approximately 15°S resulting in the formation of the southward flowing Brazil Current (BC), the western boundary current of the gyre. The eastward flowing South Atlantic current and the northward flowing Benguela current complete the circulation, delimiting the southern and eastern boundaries of the subtropical gyre, respectively (Peterson and Stramma, 1991). The dynamics in the southwestern Atlantic is dominated by the convergence of the Malvinas Current (MC), which is northward flowing and cold, with the Brazil Current, a southward flowing warm weak western boundary current (Figure 1). The region of convergence of these two currents, called the Brazil-Malvinas Confluence (Gordon and Greengrove, 1986), exhibits complex frontal motions and patterns with the simultaneous presence of warm and cold rings and eddies. Observations indicate that the latitude of the Confluence changes seasonally (Matano, 1993) and has large year-to-year variability (Goni and Wainer, 2001). A very detailed study of the Brazil Current frontal variability in the Confluence region using very high resolution (4km) sea surface temperature observations during a 9-year time span (Saraceno et al., 2004) examined the very complicated surface structures associated with the BC and MC, with reported average values of SST gradients of 0.3°C/km.

The investigation of the low frequency variability of large-scale ocean features, such as gyres, is possible using sustained hydrographic and/or satellite observations. Recently, a weakening in the circulation of the North Atlantic subpolar gyre was identified using 11 years of satellite-derived sea height anomaly (SHA) and hydrographic observations (Hakkinen and Rhines, 2004), showing that the decrease in the gyre strength observed during the 1990s is consistent with changes in buoyancy fluxes over the subpolar gyre during the same period. Conversely, using 12 years of satellite altimetry and hydrographic data, evidence for a spin-up of the South Pacific subtropical gyre has been recently reported and linked with changes in Ekman pumping (Roemmich *et al.*, 2007). Satellite altimetry observations have been used in the investigation of long period upper ocean variability in the South Atlantic. For instance, large scale interannual variability has been observed in the subtropical gyre with indications of years with very strong (1993-1995) and very weak (1996-1997) circulation (Witter and Gordon, 1999). Unlike Hakkinen and Rhines (2004), this latter study showed that these interannual changes in large scale circulation are consistent with a response to wind forcing, with wind stress curl (WSC) explaining up to 45% of the low frequency variance. The variability in the transport of the MC has also been studied using altimetry observations combined with current meter data (Vivier and Provost, 1999). Their study showed that the time series of volume transport exhibits dominant periods of 50-80 days and close to 180 days, with large interannual variability. Most recently, it has been reported that the transport of this current experienced a change to a seasonal cycle (Spadone and Provost, 2009), probably due to remote wind forcing. Little energy was found at the annual period, suggesting that the MC has only a small influence on the annual migration of the Confluence. Most of the variability in the South Atlantic Ocean is concentrated in the region of Confluence and in the Agulhas retroflection, where the sea height and eddy kinetic energy exhibit larger values (Figure 2). Lower values of sea surface variability are also found in the center of the subtropical gyre, between 20°S and 40°S.

The objective of this work is to report observed low frequency variability in the Brazil Current front (BCF) and explore its link with observed changes in the South Atlantic subtropical gyre and wind field. The insufficient hydrographic observations available in the South Atlantic render satellite altimeters and radiometers the only observing platforms capable to investigate long term thermal and dynamical changes in the region. The 15-year long altimetry record allows analyzing the surface height and subsurface trends that could correspond to decadal signals or secular changes. In order to report these results, this manuscript is organized as follows. The data used in this work are presented in section 2. In section 3, the variability of the BCF is analyzed in terms of the separation of the BC from the continental shelf break using sea surface temperature and sea height anomaly fields, and using synthetic Lagrangian drifters. The low-frequency variability of the BCF is then compared with long-term changes of geostrophic transport of the BC and MC. In section 4, these changes are linked to observed changes in the subtropical gyre extension and their geographical dependence are reported through analysis of trends of SHA, Eddy Kinetic Energy (EKE), sea surface temperature (SST), and wind stress. Section 5 presents the summary and conclusions.

2. Data

The temporal and spatial resolution of in situ oceanographic observations in the South Atlantic Ocean is sparse. Only satellite derived observations of SHA and SST, and reanalysis winds offer sufficient temporal and spatial resolution to study the low-frequency variability of large and mesoscale oceanographic structures, such as the subtropical gyre and the BCF. Over the subtropical oceans, adjacent altimeter groundtracks are between 100 km and 250 km apart, which are considerably larger than the internal Rossby radius of deformation (40 km), making a single satellite unable to resolve the mesoscale field. For this reason, the resolution capability of satellite-derived SHA for mesoscale studies has been a matter of study (e.g. Le Traon *et al.*, 1995; Greenslade *et al.*, 1997). However, resolution of ocean mesoscale processes is improved by combining observations from at least two satellites to resolve mesoscale features in mid latitude regions (Le Traon and Ogor, 1998; Le Traon and Dibarboure, 1999).

The sea height anomaly (SHA) fields used here are produced by AVISO, with weekly resolution on a 1/4º latitude 1/4º longitude grid combining observations of the Jason1, TOPEX/Poseidon, ENVISAT, GFO, ERS1 and 2, and GEOSAT altimeters [Le Traon et al., 1998; Ducet et al., 2000]. These fields are anomalies with respect to the mean of the 1993–1999 period. The altimetric observations used to produce these gridded fields were obtained from two to four satellites throughout the period from January to December 2008. The satellite coverage guarantees that these gridded SHA fields resolve variability of the ocean surface associated with dynamical and thermal fronts, current meandering and their associated rings. The altimeter data set is used in two ways in this work: a) to investigate the position of the BCF as determined by the location of the jet of the BC, and b) to analyze the trajectory of synthetic drifters deployed in geostrophic velocity fields estimated from altimetry observations.

In the South Atlantic, four main modes of low frequency sea height variability have been identified using altimetry observations: the subtropical basin-scale mode corresponding to zonal shifts in the subtropical gyre that explains more than half of the sea level variance; the tropical mode located in the northern portion of the basin; a 2-3 year mode in the Confluence region corresponding to meridional variations of the latitude of the confluence and to variations in the regional distribution of eddy variability; and the Cape Basin mode east of South Africa (Witter and Gordon, 1999; Fetter and Matano, 2010). Furthermore, long term changes in the SHA fields provide information on the low frequency variability of the global upper ocean circulation and have been extensively used to monitor trends in sea level (e.g. Cabanes, *et al.* 2001). In the southwestern Atlantic, the SHA fields are characterized mainly by an alternation of areas of low and high values related to the motion of the Brazil and Malvinas currents and their associated fronts and meandering, and with the shedding of mesoscale rings (Goni and Wainer, 2001).

High-resolution satellite-derived SST observations are also used to study the low frequency variability of the BCF. Microwave Optimally Interpolated SST fields obtained from observations retrieved by the TMI and AMSR-E radiometers onboard the TRMM and Aqua satellites, respectively, are used for the period 1998 to 2006. These fields have a daily resolution on a 0.25 degree grid. The dataset is completed with gridded fields obtained using SST observations from the Advanced Very High Resolution Radiometer (AVHRR). These fields are produced with a resolution of 2 days on an 18 km equal-area grid to complete the period 1993 to 1997 (Ryan *et al.*, 1996). The spatial and temporal resolutions of these fields also have the capability to resolve the strong mesoscale variability in the Confluence required to detect long-term changes without aliasing.

Monthly mean surface wind stress fields from the NCEP/NCAR reanalysis project (Kalnay *et al.*, 1996) are used to explore the role of wind forcing in the long-term changes of the BCF and the SA subtropical gyre. The zonal (τ^x) and meridional (τ^y) components of the surface momentum flux are available on a T62 Gaussian grid (approximately 2×2 degree resolution) from which the surface wind stress (τ) is computed. Additionally, trajectories of satellite tracked drogued drifters in the South Atlantic during 1992-2007 are used to support some of the results obtained from the satellite-based methodologies. The drifter positions were obtained from the AOML Drifting Buoy Data Assembly Center, where the data are quality controlled and interpolated to 6-hour intervals.

3. The Brazil Current front.

3.1 Satellite estimates.

The variability of the BCF is examined in terms of the separation of the BC from the continental shelf break, i.e. the intersection of the BCF with the continental shelf break computed using sea height (SH) fields from altimetry and satellite-derived fields of SST (Figure 3). This separation point is defined as the location of the maximum SH and SST gradient along the 1000 m isobath. The SH fields are derived from the SHA gridded values described in Section 2, adding the dynamic height climatology referenced to 750 m (Conkright et al., 1998) . In both cases, the values of the gradient of SH and SST along the 1000 m isobath is smoothened using a 10th order Butterworth filter with cutoff wavelength of 500 km. This cut-off wavelength allows removing spatial gradients associated with eddies, while preserving only the SH and SST gradients associated with the BCF. The location of maximum gradient is then set from this smoother function.

Frontal locations may not always agree, possibly because they represent surface and subsurface frontal positions, obtained using SST and SH fields, respectively. The time series of the separation (Figure 4) shows strong interannual variability with annual mean amplitudes that range from 1° to 3° consistent with previous reported results (Goni and Wainer, 2001). Monthly mean values of the separation indicate that the southernmost (northernmost) positions occur in JFM (ASO). The annual and semiannual components dominate the variability of the separation. However, the southernmost location of the BCF, which is dominated by higher frequency variability associated with mesoscale features, has been reported not to exhibit a clear annual periodicity as the frontal separation (Lentini et al, 2006).

The time series of monthly values of the separation derived from SH and SST fields indicate that in the mean the frontal location derived from satellite altimetry (jet of the current) is, as expected, consistently to the north than the one derived from SST (maximum SST horizontal gradient) by approximately 0.4° (Figure 4). The monthly anomalies of the separation indicate that their location has shifted to the south during the study period (Figure 5 a, b). The least-squares trends of the separation derived from altimetry and SST fields are (-1.02 ± 0.13) degree per decade and (-0.52 ± 0.18) degree per decade, respectively. Although these values are different, they both have the same sign and the difference may be related to sampling issue or to the fact that SST is more representative of the sea surface, while SH of the water column. The uncertainty in these estimates is given by the standard error of the trend computed from the time series with the climatological annual cycle removed, considering only the dispersion of the data points and not their experimental error. Thus, this standard error represents a lower bound for the uncertainty, which would be larger if other sources of error are considered. These trends are statistically compatible within 1.6 standard errors, while statistically different from zero within at least 2.89 standard errors. The trend to the south is more evident in the separation than in the southernmost location (not shown), since the dynamics of the latter is dominated by intermittent ring shedding (Lentini *et al*, 2006). The total shift during 1993-2006 is larger than 1 degree, a magnitude several times larger than the spatial resolution of the satellite-derived SHA and SST fields, therefore making these results statistically significant. These same qualitative results were not found by Goni and Wainer (2001) because their time series extended only until 1998 and the larger changes in frontal motion started that same year.

3.2. Lagrangian Estimates.

Trajectories of Lagrangian drifters are also analyzed to investigate if the variability observed from the SST and altimetry-derived estimates can be supported with observations derived from an independent platform such as surface drifters. We used the trajectories of all drifters that traveled within a closed box located in the Brazil Current, and limited by 52°W-48°W and 34°S-32°S. These drifters were followed after entering this box and their trajectories were separated into two groups, corresponding to the periods 1993-1999 and 2000-2006, and each of them for the months of JFM and JAS. An examination of their trajectories indicates that during the months of JAS during the period 2000-2006 the trajectories are more to the south than during 1993-1999 (Figure 6). However, these results cannot be considered conclusive because there are only 49 drifters that travelled in this region, which represents a very sparse spatial coverage and low temporal resolution.

Alternatively, in order to explore dynamical changes in the confluence region we compute trajectories of synthetic drifters integrating the near-surface geostrophic velocities derived from satellite altimetry. The surface currents (u_g,v_g) are computed from geostrophy as:

$$u_g = -g\left(f\,\bar{a}^{1}\right)\partial\eta/\partial\lambda, \qquad v_g = -g\left(f\,\bar{a}^{1}\cos\lambda\right)\partial\eta/\partial\theta, \qquad (1)$$

where λ is latitude, θ is longitude, *g* is gravity, *f* is the Coriolis parameter, *a* is the Earth radius, and *η* is the sea height. The time-mean component of the sea surface height field, *η*, is obtained from a methodology that combines the geoid, satellite altimetry, and in situ hydrography [Rio and Hernandez, 2004]. The time-varying component is the SHA derived from satellite-altimetry observations. Since this velocity field is purely geostrophic, the particle trajectories do not simulate surface drifters, but drifters flowing in the subsurface right below the Ekman layer.

The synthetic drifter trajectories are integrated using a fourth order Runge–Kutta method with a fixed 7-day time step and a linear interpolation scheme. Every 4 weeks starting in Jan 1, 1993, 230 drifter particles were released from a 2ºx2º box centered at 50ºW 34.5ºS and integrated for 2 years (Figure 7). This box is located off the coast of South America and within the location of the time-mean jet of the Brazil Current and upstream from the Brazil-Malvinas confluence, guaranteeing that most synthetic drifters will be trapped in the Brazil Current. The particles initially follow the Brazil current southward into the confluence region. Some particles recirculate close to the box and never reach the confluence. The 2-year length of the integration allows some of the particles to follow the large-scale circulation of the South Atlantic subtropical gyre (Figure 7). A few trajectories follow the South Atlantic current and circulate around the gyre reaching back to the Brazil Current during the 2-year integration. However, the majority of the trajectories recirculate closer to the confluence. Additionally, the trajectories show variability associated with mesoscale features of the circulation captured by the altimetric observations.

The particle trajectories are used to compute the density of particle locations as the number of drifters that traveled over each 1/4ºx1/4º bin of the domain throughout a year. Each yearly map of particle densities includes drifter trajectories corresponding to 13 releases of particles simulated throughout that year. Over a given year, the spatial distribution of the density of particles captures the large-scale circulation of the South Atlantic subtropical gyre showing values of about 100 particles per 1/4ºx1/4º bin near the center of the gyre and very low values at the boundaries of the gyre (Figures 7a and 7b). The difference in particle densities between years 2006 minus 1993 shows an increase in the number of particles reaching southern locations in the confluence region, therefore providing more evidence for a southward shift of the BCF (Figure 7c).

3.3. Brazil and Malvinas current transports.

Some theoretical and modeling studies have successfully explained why the separation of the BC from the continental margin is located north of the zero WSC contour and is, instead, governed by the relative strength of the MC and the BC (Veronis, 1973; Matano, 1993). Following these arguments, changes in the geostrophic transport of the BC and MC are analyzed to investigate a possible link with the observed BCF trend.

The BC transport across a descending altimeter groundtrack is estimated using the SHA values added to the mean dynamic height referenced to 1000 m, following the work of Goni and

Wainer (2001). The time series of the geostrophic transport of the BC shows strong annual and semi-annual variability with annual mean amplitudes that range from 5 to 20 Sv. The annual cycle is less clear in the MC (Vivier and Provost, 1999a and 1999b). Both time series show large interannual variability with year-to-year changes up to 10 Sv consistent with these previous studies. The time series of the BC transport (Figure 5c) does not exhibit a long-term trend compared with the time series of BC separation. The least-squares trend of (−0.14 ± 0.09) Sv per decade is not only negligible, but also statistically compatible with zero trend at about 1 standard error. This is consistent with no change in the Sverdrup transport of the South Atlantic subtropical gyre as shown by the spatial patterns of the WSC trends (Figure 5d), which shows no large-scale long-term changes.

Studies have shown that the MC transport has a minor role in the annual and interannual variability of the Confluence region (Vivier and Provost, 1999; Goni and Wainer, 2001). A shift from a semiannual to a seasonal cycle during year 2000 was reported in the transport of this current (Spadone and Provost, 2009) probably due to remote wind forcing. This longer time series shows a least-squares trend of (−0.05 ± 0.11) Sv per decade, which is also compatible with zero trend at about 0.5 standard error. Ultimately, the absence of long-term changes in transport of the BC and MC suggests a different physical mechanism driving the observed southward trend of the BC separation.

4. The South Atlantic subtropical gyre.

Changes in the subtropical gyre circulation are reported and analyzed in order to explore potential links with the observed southward motion of the BCF. The subtropical gyre is characterized by the anticyclonic motion of the upper layers. The dynamic center of the gyre is located where the dynamic height is maximum, with isotherms deepening towards this center. Weekly fields of dynamic height are used to investigate the variability of this gyre. The dynamic height is computed by adding the altimetry-derived time-varying SHA fields with the mean dynamic height field referenced to 1000 m (Conkright, *et al.*, 1998). The contour of dynamic height of 135 cm is used to monitor changes in the interior of the gyre and this selection does not have influence on the qualitative results presented here. The extension of the interior of the gyre is estimated by the area within the 135 cm dynamic height contour. The mean dynamic height is computed within the region delimited by this contour and has values ranging from 137 to 145 cm during the study period. This parameter shows a positive trend of (1.44 ± 0.14) cm per decade with a marked increase around 2001. The annual mean extension of the gyre exhibits large internannual variability with values ranging from 5.3 to 8.6×10^{6} km^2. The panels in Figure 9 show the mean extension of the gyre in June 1993 (blue contour), June 2006 (red contour) and 1993-2006 mean (green contour). The interannual variability of the gyre is superimposed on an uninterrupted positive trend since 1993, with an average increase of $(1.72 \pm 0.10)\times10^{6}$ km^2 per decade. During the study period the area of the subtropical gyre increased by 24×10^{6} km^2.

Least-squares linear trends estimated for each grid point of the SHA, EKE, SST and wind stress fields in the South Atlantic are used to analyze the spatial structure of the gyre changes during 1993-2006. The mean value of the SHA trend is approximately 3.0 cm per decade, with extreme SHA trend values of −6.4 and 21.1 cm per decade found in the southwest tropical

Atlantic (Figure 9a). The SHA trends over the South Atlantic are significant to the 95% level. Sea height changes are mainly due to steric effects and mass changes (e.g. fresh water fluxes). Long-term SHA trends are assumed here to mostly correspond to changes in steric sea level and, therefore, heat storage, as supported by previous research (Willis *et al.*, 2004). The region between 30°S and 40°S in the southern portion of the subtropical gyre exhibits the largest trends, which are indicative of a change in upper ocean thermal conditions.

The geostrophic EKE is also computed from the altimetry fields as $(g^2/2f^2)(\eta_x^2+\eta_y^2)$, where g is the acceleration of gravity, f is the Coriolis parameter, and η_x and η_y are the zonal and meridional SHA gradients, respectively. The trend of EKE for the same period shows extreme values of −230 and 291 cm^2/s^2 per decade (Figure 9b). These EKE trends over the region of study are significant to the 70% level. This lower significance is consistent with the inherently noisy character of the EKE compared with SHA. The region between 30°S and 40°S in the southern portion of the subtropical gyre exhibits the largest trends, which are indicative of a change in upper ocean dynamic conditions.

The trend of SST is determined for the same period using fields from the NOAA Optimal Interpolation SST analyses (Reynolds and Smith, 1994). Unlike the trends of SHA, which are positive almost everywhere, the SST trends show a large scale pattern of positive and negative values approximately coincident with the location of the 135 cm dynamic height contour, the proxy used here for the interior of gyre. In the subtropical gyre and in the Confluence region the trends of SST exhibit extreme values of −0.83 and 0.89°C per decade (Figure 9c) with a clear basin-wide spatial pattern, where positive trends are located in the interior of the gyre, the

Zapiola anticyclone, and Benguela Current regions. SST trends are significant to the 60% level, consistent with the noisier nature of SST compared with SHA.

Trends of wind stress (Figure 9d, arrows) and WSC (Figure 9d, colors) are used to explore possible links between these parameters and the observed variability in the subtropical gyre and the BCF. The trends of wind stress are very small in most of the area occupied by the subtropical gyre, except for the band south of the gyre between 32°S and 50°S, where easterly trends (i.e. weakened westerlies) are verified with extreme values of -0.020 and -0.014 Pa per decade. This area of negative τ^x trends is located east of the Confluence region in the region of largest changes in SHA. The trends of the wind stress components and curl are significant to the 60% level.

The mean dynamic height contours of 135 cm corresponding to June 1993 and June 2006 support the results found in the SHA and EKE trends showing that the changes in the gyre are not spatially uniform. Excluding the Agulhas retroflection region, the trends of SHA and EKE appear to be larger in the Confluence region, around the permanent Zapiola anticyclone, and in the slanted region between 30°S and 35°S (Figure 9a and 9b). The trends in SHA indicate that the Zapiola gyre increased its surface height, while the positive trends in EKE on the edges of the anticyclone indicate a possible strengthening. The largest trends in SHA found in the region between 30°S and 35°S are indicative of a deepening of the isotherms. This corresponds to a change in dynamic height that is concurrent with an alternation of positive and negative EKE trends, south and north of the Confluence region, indicating that the main circulation in this area of the gyre has shifted to the south.

In the subtropics, the variability of the sea height is approximately proportional to the variability of the depth of the isotherms within the main thermocline waters and to the upper ocean heat storage below the mixed layer (e.g. Meyer *et al*, 2001). Therefore, the increase in SHA is equivalent to an increase in upper ocean heat storage below the mixed layer. Trends in SST may also be indicative of a change in upper ocean heat storage in the mixed layer of the subtropical gyre. Therefore, these results are consistent with a warming of the water column between the sea surface and the main thermocline. The negative trend in the wind stress field at approximately 30°S (Figure 9d) implies slower westerly winds over the southern boundary of the subtropical gyre, possibly increasing the heat storage of the upper ocean by reducing latent and sensible heat fluxes. The spatial pattern of the WSC trend (Figure 9d), with a positive (negative) anomaly south (north) with respect to the climatological zero-curl line, indicates a southward shift of this line, which drives a southward shift of the confluence region. Clearly, the mechanisms invoked to explain the annual-mean location of the separation of the BC can partly explain the long-term trends of the separation of the BCF from the continental shelf break. On the other hand, the expansion of the gyre may require a more complex analysis including a surface heat budget study.

5. Conclusions.

A 15-year long record of satellite observations of sea height and sea surface temperature is used to monitor the low frequency variability of the Brazil Current front during 1993-2008. Given the record length, it cannot be assessed whether these trends may be associated with long-period changes or with secular trends. When the 135 cm contour of dynamic height referenced to 1000 m is used as representative of the interior of the gyre, its mean annual extension increased by approximately 40% during the study period. These changes are concurrent with the observed southward shift of the BCF. Results indicate that the separation of the BC shifted southward by approximately 1.5 degrees in latitude during the 1993-2008 period. This change of more than 100 km, represents an important departure from the mean location of the frontal region compared, for instance, with the seasonal cycle that exhibits changes of approximately 400 km. This shift cannot be explained by changes in the relative transport between the BC and MC, as proposed by theory and simple models. The analysis of trajectories of surface drifter observations cannot be used to conclusively support these results due to the low number of drifter observations. However, trajectories of synthetic drifters generated using altimetry-derived geostrophic currents indicate that there is a shift to the south of the separation of the BCF from the continental shelf break. The positive trends found south of the line of zero WSC agrees with the findings that the BCF is shifting to the south. Positive trends in the SST in the region of the subtropical gyre and the BCF, together with positive trends in the SHA, suggest an increase in the upper ocean heat content, which can be partly responsible for the observed increase in the extension of the gyre. As records of satellite observations become longer, the nature of these signals will be more clearly understood. Ultimately, the attribution of these changes can only be attempted through comprehensive numerical experiments using state-of-the-art ocean models. Attribution of the low frequency variability of the BC front will ultimately contribute to improved understanding of the upper ocean circulation in the SA and its link with climatic signals and the global ocean circulation.

Acknowledgements

The altimeter products were produced by Ssalto/Duacs and distributed by AVISO, with support from CNES. Microwave OI SST data are produced by Remote Sensing Systems and sponsored by National Oceanographic Partnership Program (NOPP), the NASA Earth Science Physical Oceanography Program, and the NASA REASoN DISCOVER Project. Data are available at www.remss.com. One degree resolution SST data are from NOAA Optimal Interpolation SST analyses. NCEP Reanalysis data provided by the NOAA/OAR/ESRL PSD from their web site at http://www.cdc.noaa.gov/. Drifter data are from the NOAA/AOML Drifter Assembly Center (http://www.aoml.noaa.gov/phod/dac/gdp.html). The authors thank Dr. Shenfu Dong for providing constructive comments. This work is supported by the NOAA Climate Program Office.

Beron-Vera F. J., M. J. Olascoaga, and G. J. Goni, 2008. Oceanic mesoscale eddies as revealed by Lagrangian coherent structures, Geophys. Res. Lett., 35, L12603, doi:10.1029/2008GL033957.

Biastoch, A., C. W. Boning, and J. R. E. Lutjeharms, 2008. Agulhas leakage dynamics affects decadal variability in Atlantic overturning circulation, *Nature, 27*, 489-492.

Cabanes, C., A. Cazenave, and C. Le Provost, 2001. Sea Level Change from Topex-Poseidon Altimetry for 1993-1999 and Possible Warming of the Southern Oceans, *Geophys. Res. Lett.*, 28(1), 9-12.

Conkright, M. E., Levitus, S., O'Brien, T., Boyer, T. P., Stephens, C., Johnson, D., Baranova, O., Antonov, J., Gelfeld, R., Rochester, J., Forgy, C., 1998. World ocean database 1998 CD-ROM data set documentation, Version 2.0. NODC Internal Report 14, 116pp.

Dong, S., S. Garzoli, M. Baringer, C. Meinen, and G. Goni, 2009. Interannual variations in the Atlantic meridional overturning circulation and its relationship with the net northward heat transport in the South Atlantic, Geophys. Res. Let., 36, L20606, doi:10.1029/2009/GL039356.

Donners, J., S. S. Drijfhout, W. Hazeleger, 2005. Water mass transformation and subduction in the South Atlantic, *J. Phys. Oceanogr.,* 35, 1841-1860.

Ducet, N., P.-Y. LeTraon, and G. Reverding, 2000. Global high-resolution mapping of ocean circulation from TOPEX/Poseidon and ERS-1 and –2. *J. Geophys. Res.*, *105*(C8), 19,477-19,489.

Fetter, A. and R. Matano, 2010. The remotely and locally wind-forced variability of the South Atlantic Ocean, *Deep Sea Res.*, in preparation.

Garzoli, S.L., and M.O. Baringer, 2007. Meridional heat transport determined with expendable bathythermographs, Part II: South Atlantic transport. *Deep-Sea Research, Part I*, 54(8):1402-1420.

Garzoli, S. L., and Z. Garraffo, 1989. Transports, frontal motions and eddies at the Brazil-Malvinas currents confluence, Deep Sea Res., Part A, 36, 681-703.

Goni, G. J., S. Kalmholtz, S. L. Garzoli, and D. B. Olson, 1996. Dynamics of the Brazil-Malvinas Confluence based upon inverted echosounders and altimetry, *J. Geophys. Res.,* 101, 16273-16289.

Goni, G. J. and I. Wainer, 2001. Investigation of the Brazil Current front variability from altimeter data, *J. Geophys. Res.,* 106, 31117-31128.

Goni, G., S. Garzoli, A. Roubicek, D. Olson and O. Brown, 1997. Agulhas Rings Dynamics from TOPEX/POSEIDON Satellite Altimeter Data. *J. Mar. Res*. , 55, 861-883.

Gordon, A. L. and C. L. Greengrove, 1986. Geostrophic circulation of the Brazil-Falkland Confluence, *Deep Sea Res.,* Part A, 33, 573-585.

Greenslade, D. J. M., D. B. Chelton, and M. G. Schlax, 1997. The midlatitude resolution capability of sea level fields constructed from single and multiple satellite altimeter datasets, *J. Atmos. Oceanic Technol.*, **14**, 849–870.

Hakkinen, S., and P. B. Rhines, Decline of Subpolar North Atlantic circulation in the 1990s, 2004. *Science*, 304, 555-559.

Kalnay E, and coauthors, The NCEP/NCAR 40-year reanalysis project, 1996. *Bull. Amer. Meteor. Soc.*, 77, 437-470.

Le Traon, P. Y., P. Gaspar, F. Bouyssel, and H. Makhmara, 1995. Using TOPEX/Poseidon data to enhance ERS-1 data, *J. Atmos. Oceanic Technol.*, **12**, 161–170.

Le Traon, PY, F. Nadal and N. Ducet, 1998. An Improved Mapping Method of Multi-Satellite Altimeter Data, *J. Atmos Ocean Tech*, 25, pp. 522-534.

Le Traon, P.-Y. and F. Ogor, 1998. ERS-1/2 orbit improvement using TOPEX/POSEIDON: the 2 cm challenge, *J. Geophys. Res.*, **103**, 8045-8057.

Le Traon, P.-Y. and G. Dibarboure, 1999. Mesoscale mapping capabilities of multiplesatellite altimeter missions, *J. Atmos. Oceanic Technol.*, **16**, 1208-1223.

Le Traon, P.Y., F. Nadal, and N. Ducet, 1998. An improved mapping method of multisatellite altimeter data, *J. Atmos. Oceanic Technol.*, *15*, 522–534.

Lentini, C., G. Goni, and D. Olson, 2006. Investigation of Brazil Current rings in the Confluence region, J. Geophys. Res., 111, doi:10.1029/2005JC002988.

Matano, R. P., On the separation of the Brazil Current from the coast, 1993. *J. Phys. Oceanogr.*, **23**, 79–90.

Mayer D., R. Molinari, M. Baringer and G. Goni, 2001. Transition regions and their role in the relationship between sea surface height and subsurface temperature structure in the Atlantic Ocean, *Geophys. Res. Let*., **28,** 3943-3946.

Peterson, R.G. and L. Stramma, 1991. Upper-level circulation in the South Atlantic Ocean, *Progress in Oceanography*, 26, 1-73.

Reynolds, R. W. and T. M. Smith, 1994. Improved global sea surface temperature analyses. *J. Climate*, 7, 929-948.

Rio, M.-H., and F. Hernandez, 2004. A mean dynamic topography computed over the world ocean from altimetry, in situ measurements, and a geoid model, *J. Geophys. Res.*, *109*, C12032. doi:10.1029/2003JC002236.

Roemmich, D., J. Gilson, R. Davies, P. Sutton, S. Wijffels, and S. Riser, 2007. Decadal spin up of the deep subtropical gyre in the South Pacific, *J. Phys. Oceanogr.*, 37, 162– 173.

Ryan, E. H., A. J. Mariano, D. B. Olson, R. H. Evans, 1996. Global Sea Surface Temperature and Currents, *Eos Transactions*, AGU, 77 (46).

Saraceno, M., C. Provost, A. R. Piola, J. Bava, and A. Gagliardini, 2004. Brazil Malvinas Frontal System as seen from 9 years of advanced very high resolution radiometer data, J. Geophys. Res., 109, C05027, doi:10.1029/2003JC002127.

Spadone, A., and C. Provost, 2009. Variations in the Malvinas Current volume transport since October 1992, J. Geophys. Res., 114, C02002, doi:10.1029/2008JC004882

Veronis, G., 1973. Model of world ocean circulation, I: Wind-driven, two-layer. *J. Mar. Res.*, **31**, 228-288.

Vivier, F and C. Provost, 1999. Volume transport of the Malvinas Current: Can the flow be monitored by TOPEX/POSEIDON?, *J. Geophys. Res.*, 104, 21105-21122.

Vivier, F. and C. Provost, 1999a. Direct velocity measurements in the Malvinas Current. *Journal of Geophysical Research*, **104**, 21083-21103.

Vivier, F. and C. Provost, 1999b. Volume transport of the Malvinas Current: Can the flow be monitored by TOPEX/POSEIDON ? *Journal of Geophysical Research*, **104**, 21105-21122

Vivier, F, C. Provost and M. P. Meredith, 2001. Remote and Local Forcing in the Brazil-Malvinas Region. *J. Phys. Oceanogr.,* 31, 892-913.

Willis, J. K., D. Roemmich, and B. Cornuelle, 2004. Interannual variability in upper ocean heat content, temperature, and thermosteric expansion on global scales, *J. Geophys. Res.*, 109, C12036, doi:10.1029/2003JC002260.

Witter, D., and A. Gordon, 1999. Interannual variability of South Atlantic circulation from 4 years of TOPEX/POSEIDON satellite altimeter observations, *J. Geophys. Res.*, 104(C9), 20927-20948.

FIGURES

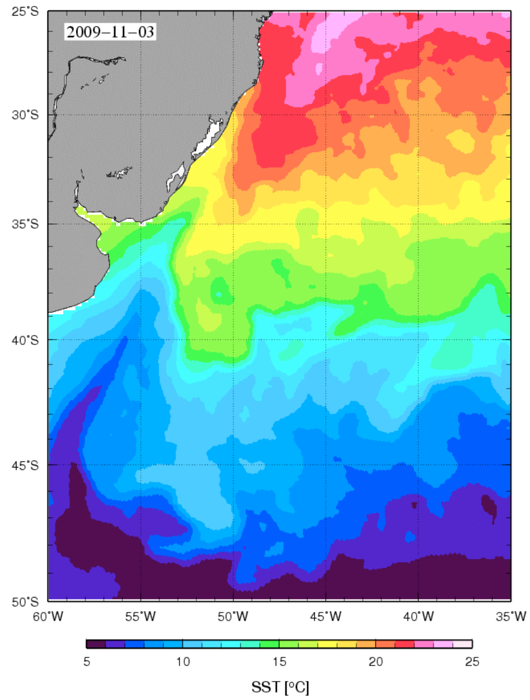

Figure 1. SST composite for 3 November 2005 exhibiting a southern incursion of the southward flowing warm Brazil Current. The region of convergence between the Brazil Current and the cold northward flowing Malvinas Current is called the Confluence region.

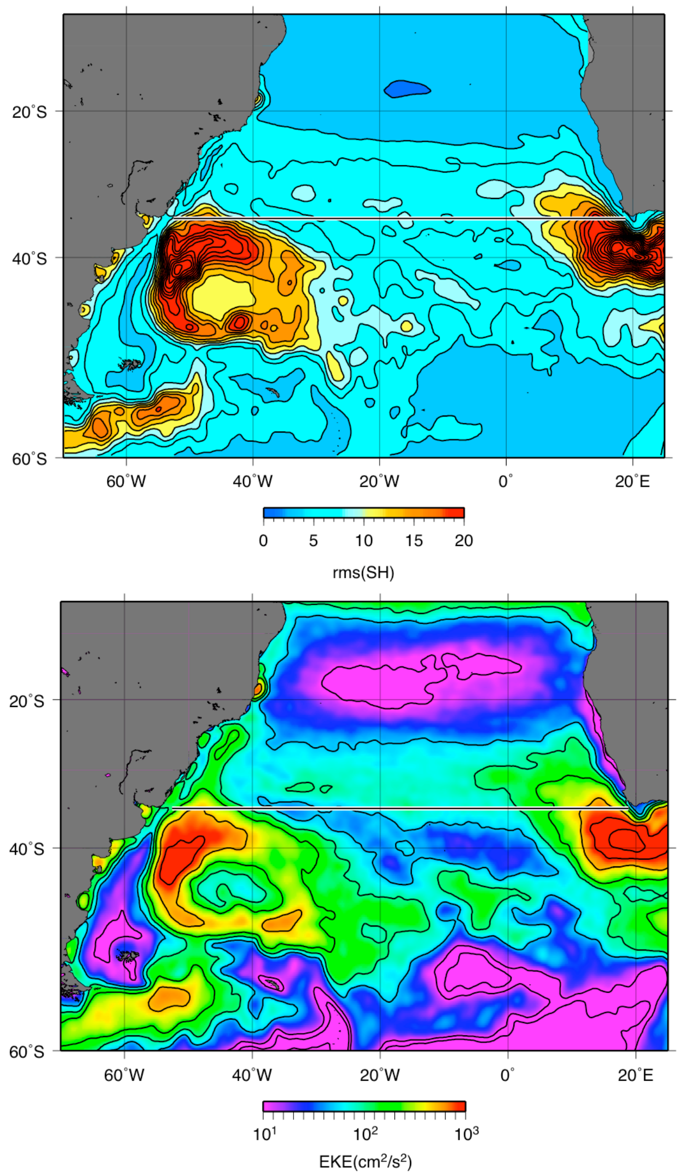

Figure 2. Satellite altimetry-derived rms of sea height (SH) and eddy kinetic energy (EKE) in the South Atlantic Ocean.

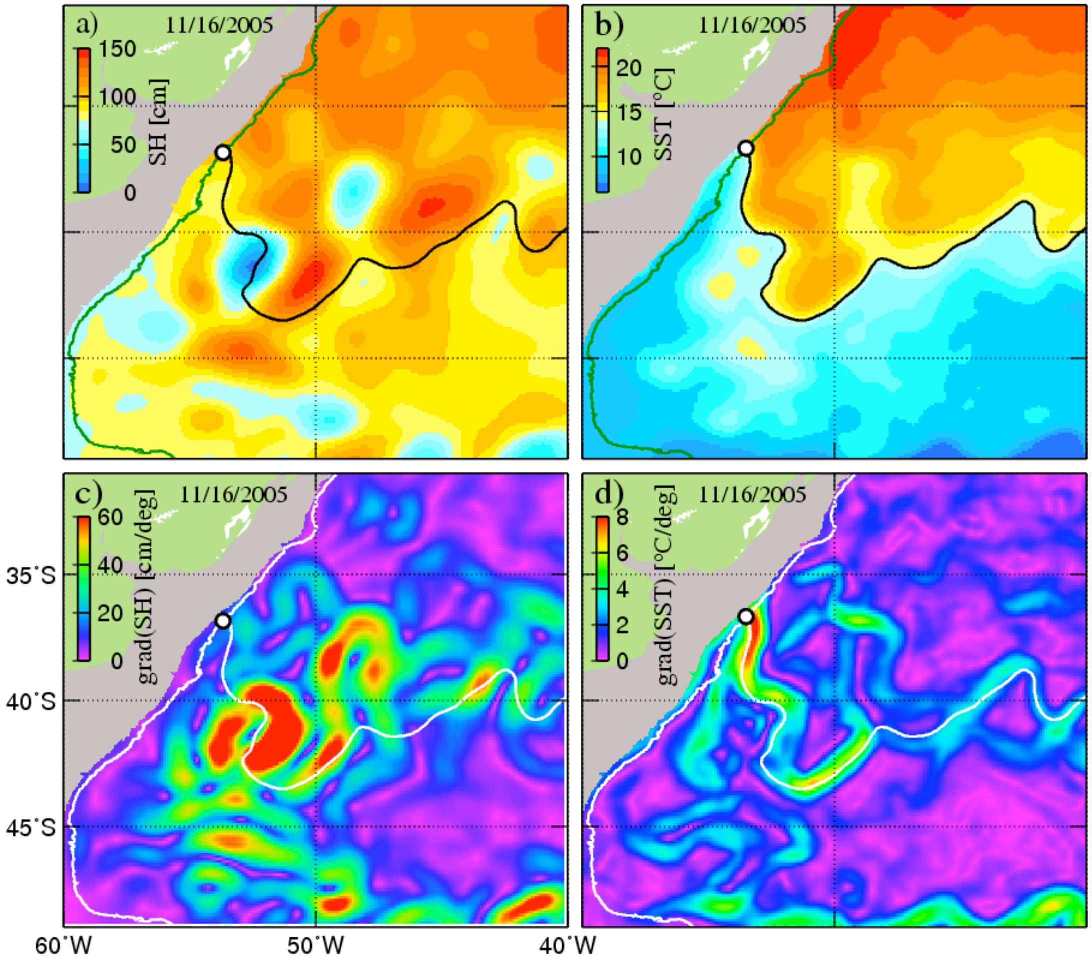

Figure 3. Fields of (right) sea height (SH) and sea surface temperature (SST) corresponding to November 16, 2005. (bottom) the horizontal gradients of the fields above. The continental shelf break, the location of the front as determined from the sea surface temperature field, and (white circle) the separation of the front from the continental shelf break are shown.

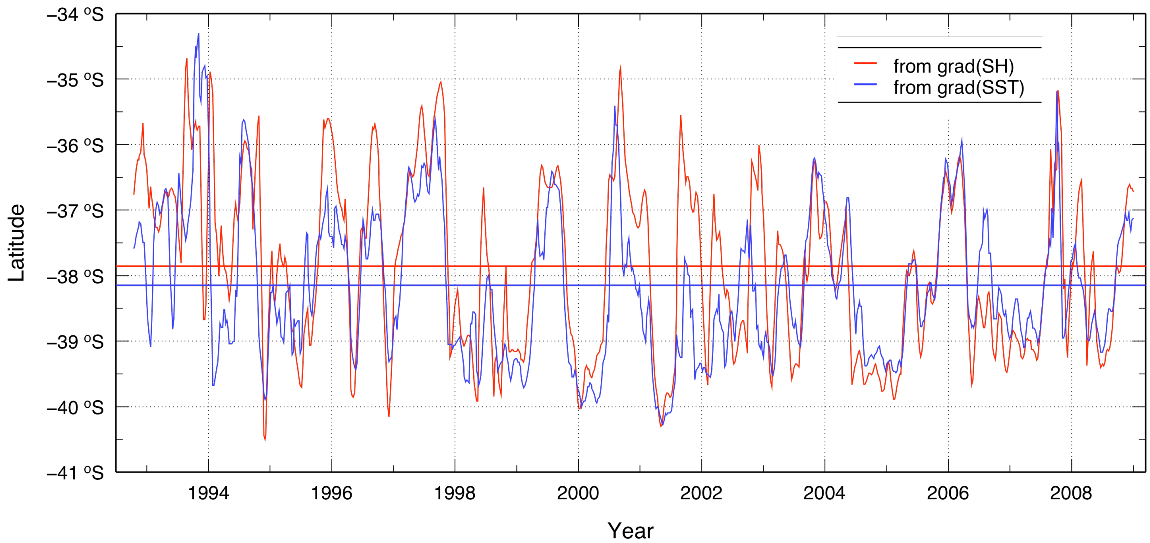

Figure 4. Time series of the separation of the Brazil Current front from the continental shelf break (1000m isobath) computed using (red) sea height and (blue) sea surface temperature fields.

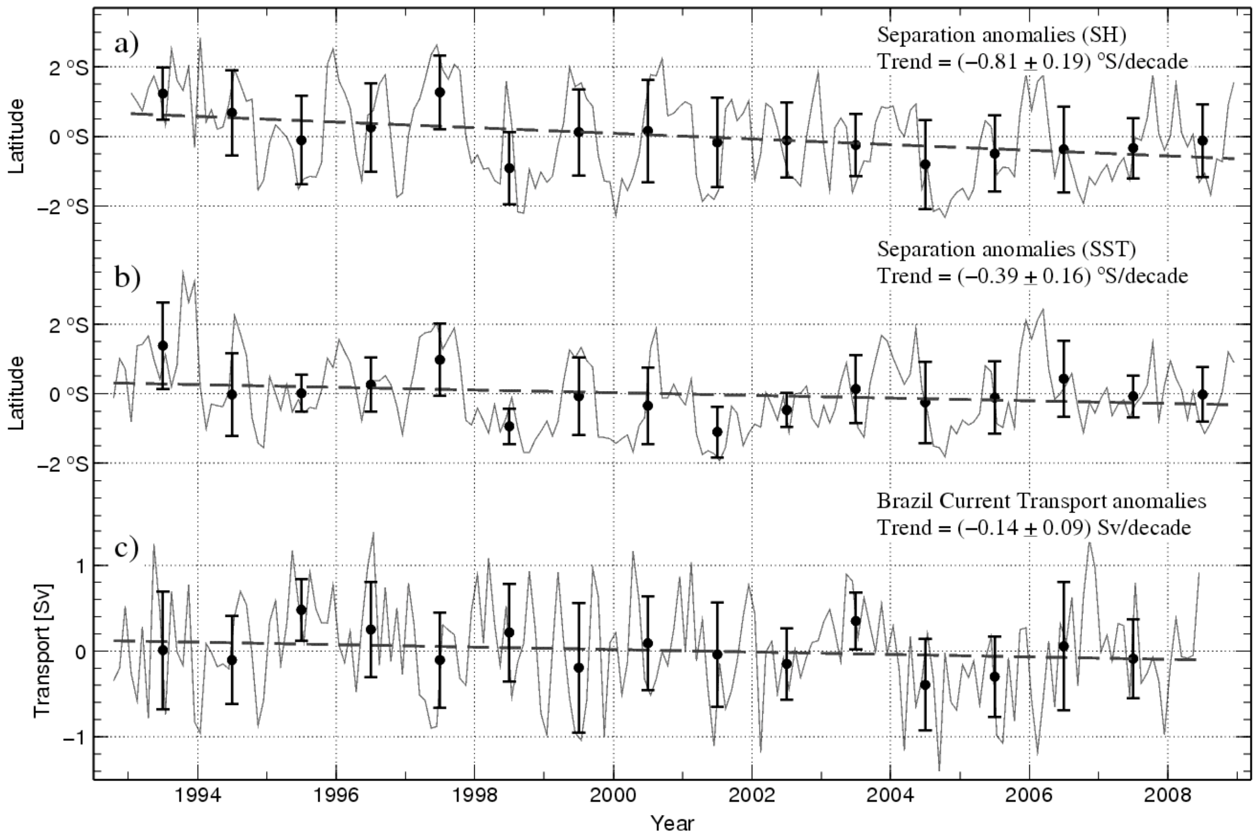

Figure 5. Monthly anomalies of the latitude of separation of the BC from the continental shelf break derived from (a) altimetry and (b) SST. (c) Monthly anomalies of geostrophic transport of the BC. The circles indicate mean annual values with their standard deviation represented by the bars. The dashed lines are the least-squares linear fit of the monthly anomalies time series, the value of the slope (trend) is indicated in the figure for each case, including the standard error.

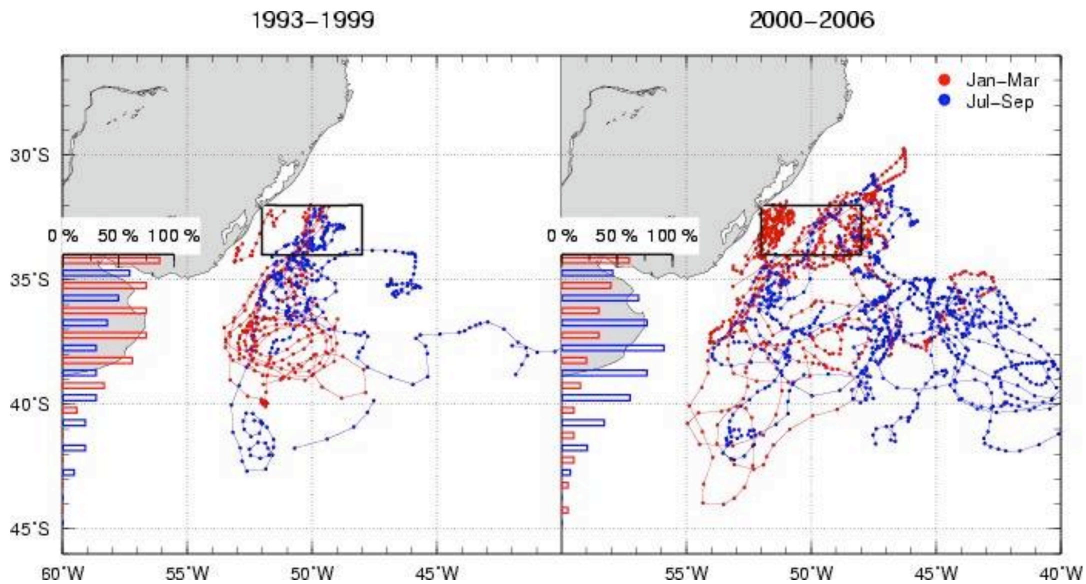

Figure 6. Surface drifter trajectories during 1993-1999 (left) and 2000-2006 (right) during January-March (red) and July-September (blue). Only trajectories for drifters traveling across the box are included. The histograms to the left of each panel indicate the percentage of the number of drifters that reach each latitude. For the period 1993-1998 there were 18 drifters and during the period 2000-2006 there were 31 drifters.

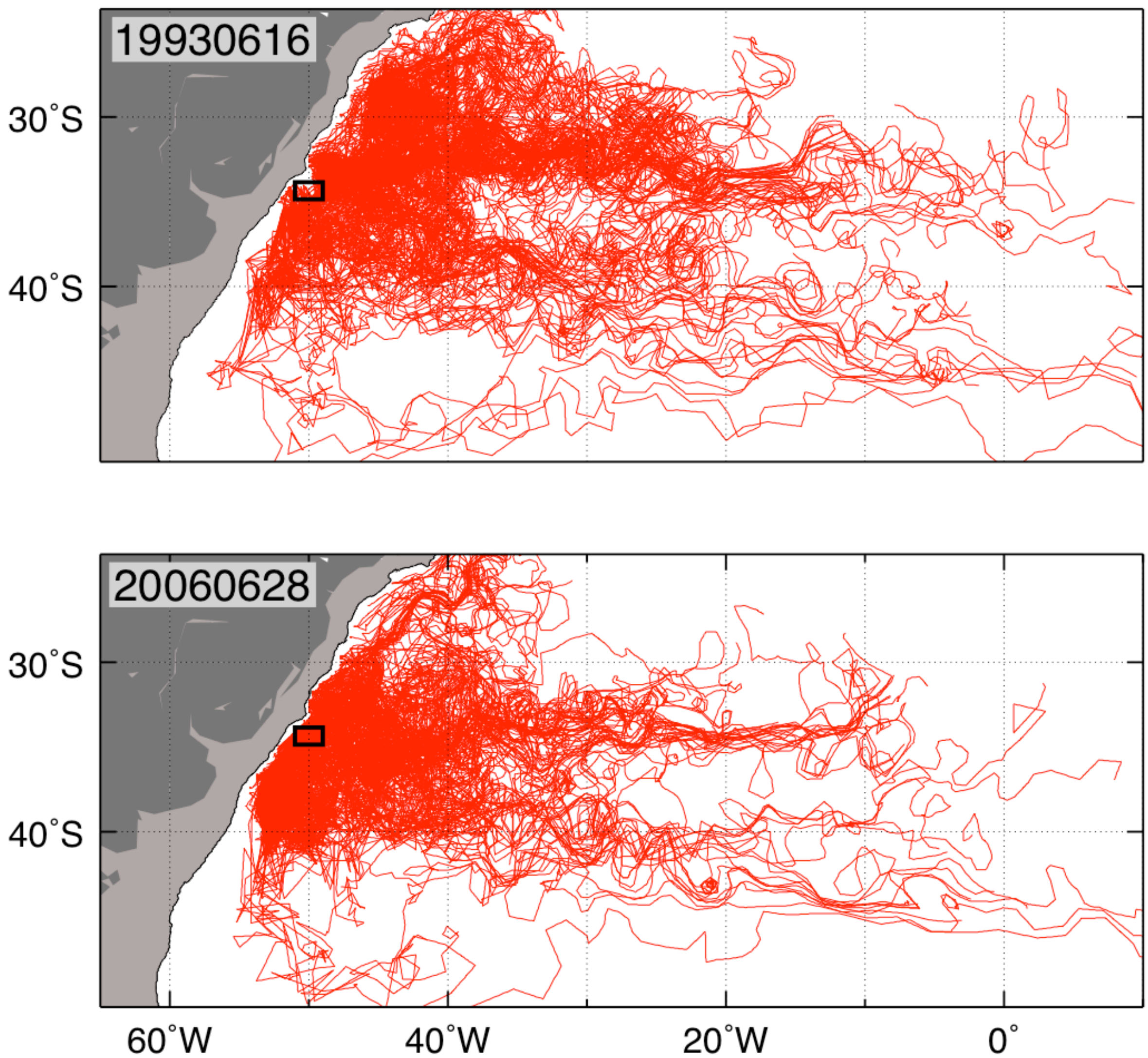

Figure 7. Trajectory of 230 synthetic Lagrangian drifters deployed on (top) June 16, 1993; and (bottom) June 28, 2006. The square corresponds to the box where the drifters were deployed. The light gray region corresponds to continental shelf and the thin black line to the 1000m isobath.

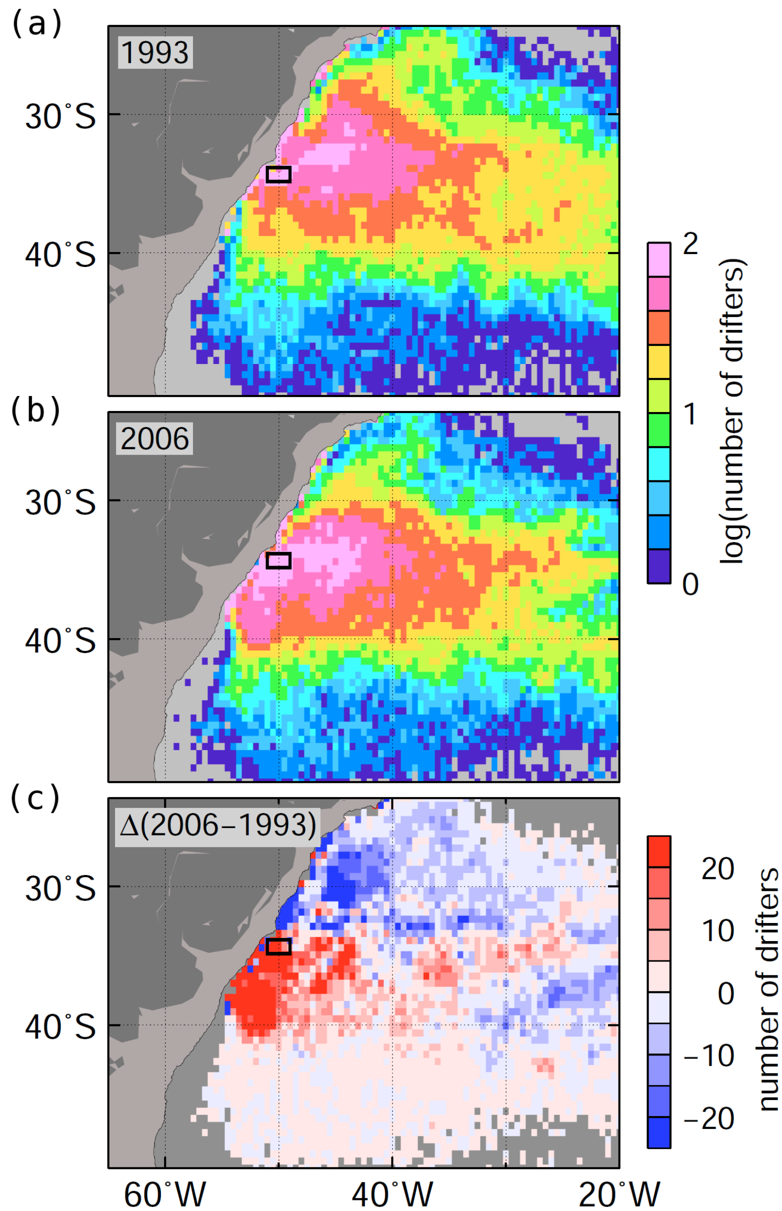

Figure 8. Density of drifter locations, expressed as the number of drifter locations on 1/4deg x 1/4deg boxes, derived from synthetic trajectories of drifters during years (a) 1993 and (b) 2006. Drifter particles are deployed every two months from the box centered at 50°W 34.5°S located off the coast of South America. The color scale is logarithmic to emphasize the strong gradients in drifter density associated with the Brazil Current front. (c) Change in density of drifter locations between years 1993 and 2006.

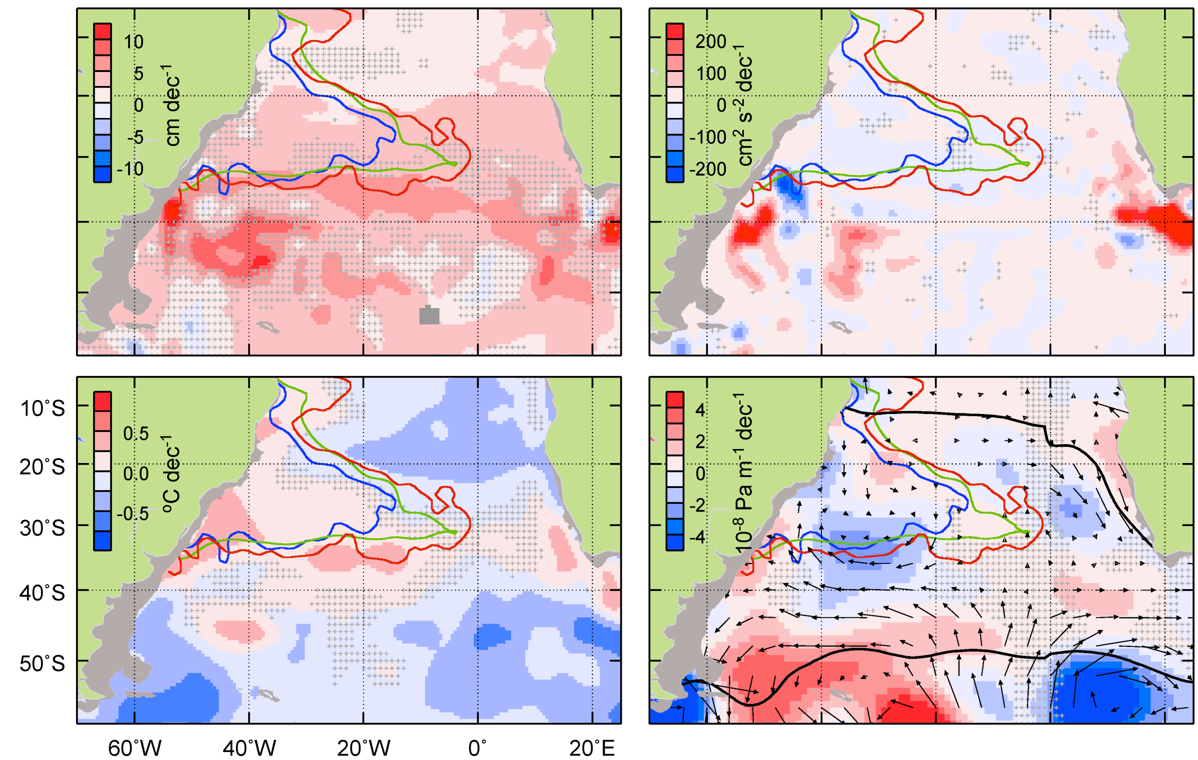

Figure 9. Linear trend of the interannual variability of (a) altimetry-derived sea height anomaly (SHA), (b) altimetry-derived eddy kinetic energy (EKE), (c) sea surface temperature (SST), and (d) wind stress curl (WSC) and wind stress (arrows), during 1993-2006. Stippling indicates linear trends that are not statistically significant to 95% for SHA and 67% for SST, EKE and WSC. The solid black line in d) indicates the climatological zero-curl contour for the period 1993-2006.